

On memory in exponentially expanding spaces

Daniel A. Roberts^a and Douglas Stanford^b

^a *Center for Theoretical Physics and
Department of Physics, Massachusetts Institute of Technology
Cambridge, MA 02139, USA*

^b *Stanford Institute for Theoretical Physics and
Department of Physics, Stanford University, Stanford, CA 94305, USA*

^adrob@mit.edu, ^bsalguod@stanford.edu

Abstract

We examine the degree to which fluctuating dynamics on exponentially expanding spaces remember initial conditions. In de Sitter space, the global late-time configuration of a free scalar field always contains information about early fluctuations. By contrast, fluctuations near the boundary of Euclidean Anti-de Sitter may or may not remember conditions in the center, with a transition at $\Delta = d/2$. We connect these results to literature about statistical mechanics on trees and make contact with the observation by Anninos and Denef that the configuration space of a massless dS field exhibits ultrametricity. We extend their analysis to massive fields, finding that preference for isosceles triangles persists as long as $\Delta_- < d/4$.

Contents

1	Introduction	1
2	Memory of initial conditions	3
2.1	Ising model on a tree	3
2.2	Gaussian model on a tree	8
2.3	Free fields in EAdS	10
2.3.1	Standard quantization	12
2.3.2	Alternate quantization	13
2.3.3	Mutual information	14
2.4	Free fields in dS	16
2.5	CFT	17
3	Configuration-space ultrametricity	19
3.1	Ising model on a tree	20
3.2	Free fields in dS	21
3.2.1	Setup	21
3.2.2	Ultra-light fields	23
3.2.3	Heavier fields	25
4	Conclusion	26
A	Super-horizon wave function in de Sitter space	27

1 Introduction

The exponential expansion of de Sitter space tends to wash away information about initial conditions [1]. This cosmic no-hair principle, which has both classical [2] and quantum mechanical [3] versions, gives inflation [4] predictive power, and may do the same for eternal inflation [5]. Cosmic no-hair can be paraphrased as follows: expectation values of quantities defined in a fixed number of regions of fixed proper size forget the initial conditions at sufficiently late time. The “fixed” qualifiers are important. Local quantities forget initial conditions, but global quantities, such as integrals of fields over the entire spatial slice, may not.

A closely related question has been studied thoroughly in the context of statistical mechanics on trees. The prototypical example, reviewed in [6], is the Ising model on an infinite tree with free boundary conditions. This system can be written via transfer matrix as a Markov problem, and an analog of cosmic no-hair follows from Markov convergence.

The more interesting question, known in the literature as the “reconstruction” or “broadcast” problem, is whether the probability distribution for a global quantity, such as the total magnetization of the spins on the leaves of the tree, depends on the value of a spin at the root. As it turns out, there is a phase transition. Below a critical T_c , the majority vote of spins at infinity tends to coincide with the root [7, 8], while, above T_c , the joint distribution for root and boundary spins is exactly a product: all memory is washed away [9].

Our first purpose in this paper will be to understand the analog of this transition, in de Sitter space [10] and Euclidean Anti-de Sitter space. As we’ll see, the temperature T_c from the Ising model corresponds to a critical value $\Delta_c = d/2$ for the dimension that characterizes the falloff of correlation functions near the boundary of dS or EAdS. It is well known that Δ_- for free fields in de Sitter never falls below $d/2$. Indeed, we’ll see that such fields always remember the initial conditions.

We’ll be more quantitative later, but for now, “remembering the initial conditions” simply means that, as the cutoff tends to infinity, a finite correlation remains between some function of the late-time configuration and early-time fluctuations. In fact, this correlation can be very large. Nonperturbative bubble nucleation can be characterized by a collection of highly non-Gaussian fields that keep track of the local vacuum index [11]. In the case where the nucleation probabilities are exponentially small, a late-time configuration will contain enough information to accurately reconstruct the entire history.

In contrast to the situation in de Sitter, free fields in EAdS can fall off faster or slower than $d/2$, depending on the choice of standard (no memory) or alternate (memory) boundary conditions [12]. The fact that this can go either way means that the memory phenomenon should have an interpretation purely in CFT terms. Indeed, one way to make the analogy is to consider a Euclidean CFT perturbed by a relevant operator at infinity. The existence of memory becomes the question of whether the statistics of functions of an order one fraction of all UV degrees of freedom are sensitive to the infrared perturbation.

Memory can also be understood in the fixed point CFT, or unperturbed (EA)dS, as a sort of failure of the central limit theorem. Limiting late-time global quantities in (EA)dS, or functions of all the UV degrees of freedom in a CFT, involve an infinite number of variables. If these variables are sufficiently independent, the distribution for the global quantity must be Gaussian. Generally, we’ll see that memory of initial conditions translates to non-Gaussian statistics for these global quantities. In the language of Gibbs states, this

is related to the existence of multiple extreme components.¹

The presence of multiple Gibbs states in the Hartle-Hawking ensemble was recently pointed out by Anninos and Denef [13], who analyzed a massless field in dS and demonstrated the existence of multiple extreme states. They went on to compute probability distributions for the distances between three field configurations, independently drawn from the Hartle-Hawking ensemble, and found a non-Gaussian, somewhat ultrametric distribution of distances. Here we will extend their analysis to positive mass fields in de Sitter, finding that the Anninos-Denef ultrametricity extends to massive fields as long as $\Delta_- < d/4$, but that the overlap distributions become Gaussian beyond this point.

The plan of this paper is as follows. In section 2, we will examine the question of memory in five different systems: first reviewing literature about the Ising model on a tree, then moving on to Gaussian fields on a tree, free fields in EAdS, free fields in dS, and general CFTs. In section 3, we will discuss the space of extreme states. We'll give a rather explicit description for the Ising model on a tree, before going on to extend Anninos-Denef ultrametricity to positive mass fields in de Sitter.

2 Memory of initial conditions

2.1 Ising model on a tree

Like many concepts in statistical mechanics, memory can be illustrated most simply with the Ising model. Consider the system on a (rooted) regular tree of degree $(p + 1)$, defined by associating a classical spin variable $s_i = \pm 1$ to each site, and taking the Boltzmann weighting with the usual pairwise Hamiltonian,

$$H = \sum_{\text{links } ij} s_i s_j. \quad (1)$$

For any finite subsystem of the tree, the number of boundary spins is of order the number of total spins, so we have to be careful about specifying the boundary conditions. For now, we will consider free boundary conditions.

We can state the criterion for the memory as follows. Write $\mathbf{s}^{(u)}$ for the collection of spins at generation u (see figure 3) in the tree, and consider the mutual information

$$I(\mathbf{s}^{(u)}; \mathbf{s}^{(0)}) = S(\mathbf{s}^{(u)}) + S(\mathbf{s}^{(0)}) - S(\mathbf{s}^{(u)}, \mathbf{s}^{(0)}) \quad (2)$$

¹We will use the term “extreme state” instead of “pure state.” And we mean extreme states in the tree/bulk, not in the CFT.

between the spins at generation u and at the root. If this quantity approaches zero as u tends to infinity, then conditioning on the value of the root spin doesn't change the distribution for the spins at $u \rightarrow \infty$. We will describe this situation by saying that the system forgets the initial conditions. On the other hand, if the mutual information is bounded from below by a positive constant as u tends to infinity, then there is correlation between the spin at the root and the collection of spins at $u \rightarrow \infty$, and we will say that there is memory in the system.

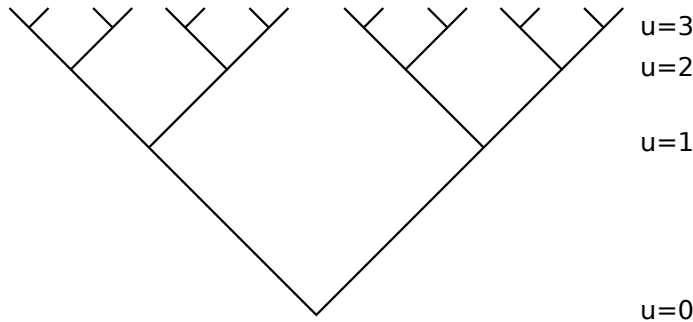


Figure 1: The time u in a $p = 2$ tree.

A priori, it might have been the case that the Ising model either always has memory, or never does. Here, we will give a heuristic argument that a transition happens at a finite value of the temperature, leaving the proof to the literature [8, 7, 9]. To make the argument, and to relate the Ising model to our other models, it will be very useful to rewrite the statistical mechanics problem defined by eq. (1) as a branching Markov process.

This is a standard application of transfer-matrix logic. The basic point is that the probability distribution for a spin at generation $(u + 1)$ depends on the spins at earlier generations only through the parent at generation u . Combined with the free boundary conditions at infinity, this means that if parent spin is up, the child is more likely to be up than down by a ratio of Boltzmann factors $e^{2/T}$. More generally, we can write the probability distribution for the spin of the child as a two component vector, obtained from that of the parent by a Markov matrix

$$G = \begin{pmatrix} 1 - \gamma & \gamma \\ \gamma & 1 - \gamma \end{pmatrix}. \quad (3)$$

where the “flip probability” γ is given in terms of the temperature by the equation

$$\frac{P(\text{child} = \text{parent})}{P(\text{child} \neq \text{parent})} = e^{2/T} = \frac{1 - \gamma}{\gamma}. \quad (4)$$

To obtain the full probability distribution for all spins at generation $u + 1$, one takes the distribution for the parent spins at generation u , assigns each parent two children, and applies the matrix G independently for each child. In particular, the evolution of the probability distribution along a given path through the tree is an ordinary Markov process. If we start out the root with spin up, the probability distribution for a given child at generation u will be evenly split between up and down, up to an exponentially decaying transient, proportional to λ^u , where $\lambda = 1 - 2\gamma$ is the second eigenvalue of the Markov matrix G . It follows that mutual information between the root and a given spin at generation u tends to zero exponentially.

Instead of looking at a particular spin, let us consider the total magnetization at generation u

$$M_u = \sum_{i=1}^{p^u} s_{(u,i)}. \quad (5)$$

It is easy to check that if the root starts with spin up, the expected value of M_u is $(p\lambda)^u$, which grows exponentially with u . One might be tempted to conclude that the total magnetization always remembers the spin of the root, but we need to be more careful. The right thing to do is to compare $(p\lambda)^u$ with the typical width of the distribution for M_u . Suppose that the system has no memory. Then distant spins at generation u will be independent, and the variance should be proportional p^u , the number of spins at generation u . We see that the assumption of no memory is consistent only if the bias in the expected total magnetization $(p\lambda)^u$ is much smaller than the square root of the variance, $p^{u/2}$. Setting these two equal gives us the critical value of λ as²

$$\lambda_c = \frac{1}{\sqrt{p}}. \quad (6)$$

If the second eigenvalue is larger than this value, the probability distribution for the total magnetization remains meaningfully biased in the direction of the initial spin. It follows that the mutual information eq. (2) cannot tend to zero at large u : the system has memory. On the other hand, if the eigenvalue is smaller than $1/\sqrt{p}$, then the bias becomes small compared to normal fluctuations, so the mutual information between M_u and the initial spin tends to zero as u grows large. Our description here was intuitive, but the result was proven rigorously in [7], using the previous work [8]. One can see the transition, as a function of λ , quite clearly in figure 2.

²This is the so called “spin-glass” transition point for the Ising model. The “Ising” transition point at $\lambda = 1/p$ is a higher temperature transition, related to the ability of the root to detect a uniform up boundary condition at infinity.



Figure 2: Sample configurations of the spins in the $p = 4$ tree after six generations, given a white initial condition at generation zero. The left panel is firmly on the “memory” side of the transition, with $\gamma = 0.05$. The middle panel is at the transition $\gamma = 0.25$, and the right panel is forgetful, at $\gamma = 0.4$.

There’s another way of understanding memory, as a breakdown of the central limit theorem. If we assume that the magnetization M_u is correlated with the value of the initial spin, then (at least at small γ), the distribution for M_u ought to be bimodal, and therefore non-Gaussian. On the other hand, if there is vanishing correlation between M_u and the initial spin, then the tree structure implies that there must also be vanishing correlation between different patches of the boundary leaves. This means that, in the limit $u \rightarrow \infty$, the random variable M_u is a sum of an infinite number of independent random variables. The central limit theorem ensures that it will have Gaussian statistics.

So far, we have considered the forgetfulness of two quantities: a given spin at late u , and the total magnetization M_u . The former never maintains memory of the initial condition at late time, while the latter does so if and only if the second eigenvalue λ is greater than $1/\sqrt{p}$. What about some other quantity? Perhaps, by constructing a more complicated function of the spins at generation u , one could find a variable that remembers the initial condition, even for $\lambda \leq 1/\sqrt{p}$. For the Ising model, this turns out not to be the case. It was proven in [9] and [6] that the mutual information itself tends to zero at late time if $\lambda \leq 1/\sqrt{p}$. For more general Markov processes on trees, the exact condition is not known. The “second eigenvalue condition” $\lambda > 1/\sqrt{p}$, also known as the “Kesten-Stigum bound” is known to be sufficient for the existence of memory, but it is not in general necessary [14].

Let us begin to translate these Ising results into the language of de Sitter space. As a first step, we can use the symmetree framework [11], which models the statistics of bubble

nucleation in eternal inflation using Markov processes on trees. The basic idea is that the exponential expansion of the tree mocks up the geometry of de Sitter. Each vertex is assigned a “color”, corresponding to the vacuum type at a given spacetime point, and these colors undergo stochastic transitions, described by Markov dynamics with some rate matrix G . The Ising model considered above corresponds, in this language, to eternal inflation with a symmetric two-vacuum landscape, and tunneling probability (per Hubble four-volume) γ . Since transitions between vacua are suppressed by tunneling factors, we should take γ to be exponentially small, making the second eigenvalue $(1 - 2\gamma)$ extremely close to one, and putting us firmly on the side of memory.

For small γ , the most likely way for reconstruction to fail is for a transition to happen in the first generation. The probability for this is order γ , so the probability of failure is suppressed by the tunnelling rate. For a bubble-nucleation setup with exponentially small tunneling rates, the late-time configuration will contain an exponentially good record of the initial condition. In fact, the late-time configuration will contain an exponentially good record of the entire history, since later vertices can be considered roots of the smaller trees growing out of them, and the same reconstruction procedure can be applied. The scale invariance of the system implies that if any memory exists, an infinite amount does.

It will be useful, in making the correspondence with the following sections, to understand the relation between eigenvalues of the rate matrix G and dimensions of fields in de Sitter space. First, we need a relation between the time variables. A $(p + 1)$ -regular tree has a spatial volume that increases with generation as p^u , while the volume of de Sitter increases with proper time t as $e^{td/\ell_{ds}}$. This gives us the identification

$$u = \frac{td}{\ell_{ds} \log p}. \quad (7)$$

Next, we would like to relate the eigenvalue of a Markov process to the scaling dimension of the corresponding field. Correlations of operators corresponding to eigenvectors of the Markov matrix fall off with proper time as λ^u . We identify this with the de Sitter behavior $e^{-\Delta_- t/\ell_{ds}}$. Combining this with eq. (7), we find

$$\Delta_- = -d \log_p \lambda. \quad (8)$$

The critical value of the Markov eigenvalue $\lambda = 1/\sqrt{p}$ therefore corresponds to a scaling dimension $\Delta_- = d/2$. A similar identification can be made in Euclidean AdS.

2.2 Gaussian model on a tree

In the previous subsection, we reviewed the memory transition for the Ising model on a tree, and discussed some implications for the symmetree model of eternal inflation. Before moving on to de Sitter and Euclidean Anti-de Sitter, we will construct a useful stepping stone: the massive Gaussian field on a tree. This model closely resembles free fields in (EA)dS, but the tree geometry will allow us to make contact with the Ising memory results, the second-eigenvalue condition in particular.

A massless Gaussian field on a regular $(p+1)$ tree was previously studied by Zabrodin [15]. We will focus on the $p = 2$ case, but add a mass. To define the model, associate to each vertex a of the tree a real field variable $\phi(a)$, and form the Boltzmann ensemble with temperature $T = 1$ and Hamiltonian (or Euclidean action)

$$H = \frac{1}{2} \sum_{\text{links}} (\delta\phi)^2 + \frac{m^2}{2} \sum_{\text{vertices}} \phi^2. \quad (9)$$

Just like the Laplacian on hyperbolic space, the discrete tree Laplacian has a gap in the spectrum, so the statistical mechanics of this system makes sense with somewhat negative mass-squared. For the $p = 2$ tree, the gap is $3 - 2\sqrt{2}$, so the action is positive as long as $m^2 > 2\sqrt{2} - 3$. When m^2 is negative, we will call it $-\mu^2$.

To get a feel for this system, we can study the equations of motion, obtained by differentiating with respect to ϕ at a particular vertex a in the tree. This gives

$$3\phi(a) - \phi(\text{child}_1) - \phi(\text{child}_2) - \phi(\text{parent}) + m^2\phi(a) = 0. \quad (10)$$

If we take a homogeneous ansatz $\phi \sim \lambda^u$, where u is time in the tree, we find two solutions,

$$\lambda_{\pm} = \frac{3 + m^2 \pm \sqrt{1 + 6m^2 + m^4}}{4}. \quad (11)$$

For small m^2 , the solutions are $\lambda_+ = 1 + m^2$ and $\lambda_- = (1 - m^2)/2$. λ_+ is greater than one for positive m^2 , so one of the solutions grows exponentially in the direction of the tree's branching. On the other hand, if $m^2 < 0$, then both branches are less than one.

It is well known that boundary conditions can be extremely important for statistical mechanics on trees. The reason is that the boundary makes up an order one fraction of the tree, for any cutoff. To be careful, we will treat the boundary vertices separately, modifying the above Hamiltonian to

$$H = \frac{1}{2} \sum_{\text{links}} (\delta\phi)^2 + \frac{m^2}{2} \sum_{\text{bulk vertices}} \phi^2 + \frac{m_{\partial}^2}{2} \sum_{\text{bdry vertices}} \phi^2. \quad (12)$$

where, in general, $m_\partial \neq m$. In order to preserve the symmetry of the tree, we would like m_∂ to be independent of the cutoff, in the sense that integrating out the boundary vertices leaves an action for a smaller region, with the same value of m_∂ . It is easy to show that this condition allows two solutions as a function of m^2 . They can be conveniently written in terms of the solutions for λ_\pm as

$$m_\partial^2 = \frac{1 - \lambda_\pm}{\lambda_\pm}. \quad (13)$$

For the special case of $m^2 = 0$, the solutions are $m_\partial^2 = 0$, corresponding to free boundary conditions, and $m_\partial^2 = 1$, corresponding to a condition that tends to suppress fluctuations. More generally, we will see that the “-” branch closely parallels the standard boundary conditions in EAdS, while the “+” branch resembles alternate boundary conditions.

Much like the Ising model, this system can be recast as a branching Markov random field. The rate matrix G along each link of the tree is a Gaussian kernel

$$G(\phi, \phi') \sim \exp \left\{ -\frac{(\phi - \phi')^2}{2} - \frac{\alpha}{2}\phi^2 + \frac{\beta}{2}\phi'^2 \right\}. \quad (14)$$

where we'll derive α and β below. This kernel assigns the probability distribution for the field value ϕ of a child vertex at generation $(u + 1)$ in terms of the probability distribution for the parent at generation u , via

$$P_{u+1}(\phi) = \int G(\phi, \phi') P_u(\phi') d\phi'. \quad (15)$$

To identify the correct values of α and β , we require that the infinite product of $G(\phi, \phi')$ along each link in the graph should equal e^{-H} . This means that we need $\alpha - 2\beta = m^2$. Another constraint comes from requiring the probability to stay normalized,

$$\int G(\phi, \phi') d\phi = 1. \quad (16)$$

Doing the Gaussian integral, this means we need $\beta = \alpha/(1 + \alpha)$. These two equations determine α and β in terms of m^2 . The equation is quadratic, so we have a choice of two solutions. Again, these can be parameterized in terms of λ_\pm as $\alpha = (1 - \lambda_\pm)/\lambda_\pm$, and $\beta = 1 - \lambda_\pm$. Since the boundary weighting implied by the Markov kernel G is $m_\partial^2 = \alpha$, we see that the upper/lower sign choice here is the same as the corresponding choice for the branch of m_∂^2 .

We conclude that the properly normalized Markov kernel is

$$G(\phi, \phi') = \frac{1}{\sqrt{2\pi\lambda_\pm}} \exp \left\{ -\frac{(\phi - \phi')^2}{2} - \frac{1 - \lambda_\pm}{2\lambda_\pm}\phi^2 + \frac{1 - \lambda_\pm}{2}\phi'^2 \right\}. \quad (17)$$

Our lesson from the previous section was that, to look for memory, we should compute the second eigenvalue of G . While G isn't a symmetric matrix, it does satisfy detailed balance, i.e. $G = ZSZ^{-1}$, where Z is diagonal and S is symmetric, so we are guaranteed to have eigenvectors and real eigenvalues. These are

$$\begin{aligned} \int G(\phi, \phi') f_n(\phi') d\phi' &= \lambda_{\pm}^n f_n(\phi) \\ f_n(\phi) &= e^{-a\phi^2} H_n(\sqrt{a}\phi) \quad a = \frac{\lambda_{\pm}}{2} + \frac{1}{2\lambda_{\pm}}. \end{aligned} \quad (18)$$

Here, H_n is the (physics convention) Hermite polynomial. One can easily check the above using the representation $H_n(x) = \frac{n!}{2\pi i} \oint \frac{dt}{t^{n+1}} e^{-t^2+2xt}$ and using Gaussian integration under the contour integral.

Now that we know the spectrum of G , there are a few points to be made. First, we see that the second eigenvalue, for either choice of boundary conditions, is equal to the corresponding falloff λ_{\pm} from the tree equation of motion. This justifies our analogy to standard and alternate quantization in EAdS: the decay of correlation functions is controlled by the second eigenvalue, which takes the “fast-falloff” value for one branch of m_{∂}^2 , and the “slow-falloff” value for the other. Second, if m^2 is positive and we pick the “+” branch, the eigenvalues of G are not bounded. This reflects the familiar fact that alternate quantization doesn't make sense for positive mass-squared. Here, we see it as a breakdown of the normalizability of the Markov matrix. Finally, and most important for our purposes, the “+” branch always has a second eigenvalue greater than or equal to the critical value $1/\sqrt{2}$,³ while the “-” branch always has an eigenvalue smaller than or equal to that value. To the extent that this is a faithful model of EAdS, we expect that with alternate quantization, simple spatial integrals of free fields near the boundary are sensitive to conditions near the center, but that with standard quantization they forget. We'll see this explicitly below.

2.3 Free fields in EAdS

The regular tree graph studied up to now can be considered a discrete version hyperbolic space. In this section, we will test the memory of free fields in continuous hyperbolic space, also known as Euclidean Anti-de Sitter. We'll define memory by analogy to section 2.1. Specifically, if the mutual information between the field variable at some fixed radius ℓ'

³Remember, we have specialized to $p = 2$ in this subsection.

and the collection of field variables near the boundary at radius ℓ stays bounded away from zero as ℓ approaches the boundary, then we will say that there is memory. Otherwise, not.

We will work with free fields, for which the statistics of different modes decouple. This makes it possible to look for memory mode-by-mode, asking whether the probability distribution for a given spatial Fourier component, near the boundary, is sensitive to conditions imposed on the same mode deep in the bulk of the space. For simplicity, we'll work with the zero mode in the \mathbf{x} directions.⁴ Whether or not memory exists depends on the choice of boundary conditions. For the “standard quantization” boundary conditions, we will find that memory doesn't exist for any allowed value of the mass, while for “alternate quantization,” we'll find that it does.

Let us work in Poincare slicing, with metric

$$ds^2 = \frac{dz^2 + dx^i dx^i}{z^2} \quad i = 1, \dots, d, \quad (19)$$

where the anti-de Sitter radius is taken to one, and $0 < z < \infty$. The action for a massive scalar field $\phi(\mathbf{x}, z)$ is

$$S = \frac{1}{2} \int \frac{d^d \mathbf{x} dz}{z^d} \left\{ z^2 (\partial_z \phi)^2 + z^2 (\partial_i \phi)^2 + m^2 \phi^2 \right\}. \quad (20)$$

We will Fourier transform this system in \mathbf{x} space, and specify to the $\mathbf{k} = 0$ component, which we'll refer to as $\varphi(z)$. The wave equation for this zero mode,

$$\partial_z^2 \varphi - \frac{d-1}{z} \partial_z \varphi - \frac{m^2}{z^2} \varphi = 0 \quad (21)$$

has two independent power-law solutions, z^{Δ_-} and z^{Δ_+} , where

$$\Delta_{\pm} \equiv \frac{1}{2} \left(d \pm \sqrt{d^2 + 4m^2} \right). \quad (22)$$

In the standard boundary conditions, we define the path integral by forcing the field to zero as $\varphi \sim z^{\Delta_+}$ near the boundary, while in alternate quantization, we allow the slower falloff $\varphi \sim z^{\Delta_-}$, but require that there be no component going like z^{Δ_+} for small z [12].

To look for memory, we will impose a condition deep in the bulk, $\varphi(z = \ell') = \varphi_{\ell'}$, and then compute the conditional probability for the zero mode at radius ℓ , $P(\varphi_{\ell} | \varphi_{\ell'})$. The un-normalized conditional probability is computed by a path integral, with standard or alternate conditions at $z \rightarrow 0$, and Dirichlet conditions $\varphi(\ell') = \varphi_{\ell'}$ and $\varphi(\ell) = \varphi_{\ell}$. The

⁴In section 2.3.3 we'll consider a general Fourier mode.

normalization is adjusted as a function of $\varphi_{\ell'}$. In computing these path integrals, we will mimic the approach of [16], splitting the computation into a “UV” piece $0 < z < \ell$, and a “visible” piece, $\ell < z < \ell'$. Up to normalization, the conditional probability is

$$P(\varphi_{\ell}|\varphi_{\ell'}) = \Psi_{UV}(\varphi_{\ell})\Psi_{VI}(\varphi_{\ell}, \varphi_{\ell'}). \quad (23)$$

In this expression, Ψ_{UV} depends on the standard/alternate boundary conditions, and we’ll handle the two cases separately below. However, Ψ_{VI} is independent of the boundary conditions. It is defined as the path integral over field configurations on $\ell < z < \ell'$, with $\varphi(\ell) = \varphi_{\ell}$ and $\varphi(\ell') = \varphi_{\ell'}$. We can do this Gaussian path integral by evaluating the action on the appropriate classical solution,

$$\Psi_{VI}(\varphi_{\ell}, \varphi_{\ell'}) \sim \exp(-S_{cl}). \quad (24)$$

Using the equations of motion and integrating by parts, the action reduces to two surface terms. The exact result for the zero mode is

$$S_{cl} = \frac{\Delta}{2} \left(\frac{\varphi_{\ell'}^2}{\ell'^d} - \frac{\varphi_{\ell}^2}{\ell^d} \right) - \frac{2\Delta - d}{2} \left(\frac{(\ell'^{\Delta}\varphi_{\ell} - \ell^{\Delta}\varphi_{\ell'})^2}{\ell^{2\Delta}\ell'^d - \ell^d\ell'^{2\Delta}} \right). \quad (25)$$

Here and in much of what follows, we will use the AdS convention $\Delta \equiv \Delta_+$ and $\Delta_- = d - \Delta$. The $\varphi_{\ell'}^2$ terms can be discarded because they are independent of φ_{ℓ} and contribute only to the normalization of $P(\varphi_{\ell}|\varphi_{\ell'})$. Keeping only the first nontrivial term in small ℓ/ℓ' , we find

$$\Psi_{VI}(\varphi_{\ell}, \varphi_{\ell'}) \sim \exp \left\{ \left(\frac{d - \Delta}{2\ell^d} \right) \varphi_{\ell}^2 + \left(\frac{2\Delta - d}{\ell^d} \right) \left(\frac{\ell}{\ell'} \right)^{\Delta} \varphi_{\ell} \varphi_{\ell'} \right\}. \quad (26)$$

If we had considered a general \mathbf{k} mode, instead of the zero mode, the expression would be similar, but would involve complicated combinations of Bessel functions. We’ll have more to say about this below.

2.3.1 Standard quantization

To compute Ψ_{UV} , let us first consider standard boundary conditions, where $\varphi(z) \rightarrow 0$ as z^{Δ} . The UV wave function is defined as a path integral over field configurations respecting this condition at the boundary, and matching $\varphi(\ell) = \varphi_{\ell}$. The result is [17]

$$\Psi_{UV}(\varphi_{\ell}) \sim \exp \left\{ - \left(\frac{\Delta}{2\ell^d} \right) \varphi_{\ell}^2 \right\}. \quad (27)$$

Taking the product of wave functions as in eq. (23), we get the conditional distribution, up to normalization, as

$$P(\varphi_{\ell}|\varphi_{\ell'}) \sim \exp \left\{ \left(- \frac{2\Delta - d}{2\ell^d} \right) \left(\varphi_{\ell} - \left(\frac{\ell}{\ell'} \right)^{\Delta} \varphi_{\ell'} \right)^2 \right\}. \quad (28)$$

To assess whether this distribution has memory or not, we will fix ℓ' and let ℓ tend to zero, asking whether significant correlation remains between the variables φ_ℓ and $\varphi_{\ell'}$. It is clear from the distribution that the width for φ_ℓ is proportional to $\sim \ell^{\frac{d}{2}}$, and the shift in the direction of $\varphi_{\ell'}$ scales as $\sim \ell^\Delta$. Since Δ is always greater than or equal to $d/2$, the width becomes large compared to the shift, so the variables lose correlation as ℓ tends to zero: there is no memory. This is very analogous to the Ising model above the memory transition temperature, where the variance in the magnetization grows large compared to the bias due to a particular initial condition.

2.3.2 Alternate quantization

Next, we consider the alternate boundary conditions, $\varphi(z) \sim z^{d-\Delta}$. This changes the path integral that defines Ψ_{UV} , and we find

$$\Psi_{UV} \sim \exp \left\{ - \left(\frac{d-\Delta}{2\ell^d} \right) \varphi_\ell^2 \right\}. \quad (29)$$

With this wave function, we see from (26) that the φ_ℓ^2 term will cancel in the product $\Psi_{UV}\Psi_{VI}$. Thus, we need to go back to the Ψ_{VI} computation and keep a higher order terms in ℓ/ℓ' . We find

$$\Psi_{VI} \sim \exp \left\{ \left(\frac{d-\Delta}{2\ell^d} \right) \varphi_\ell^2 + \left(\frac{d-2\Delta}{2\ell^d} \right) \left(\frac{\ell}{\ell'} \right)^{2\Delta-d} \varphi_\ell^2 + \left(\frac{2\Delta-d}{\ell^d} \right) \left(\frac{\ell}{\ell'} \right)^\Delta \varphi_\ell \varphi_{\ell'} \right\} \quad (30)$$

We now take the product with Ψ_{UV} , and complete the square, freely adding a term proportional to $\propto \varphi_{\ell'}^2$. The result is

$$P(\varphi_\ell | \varphi_{\ell'}) \sim \exp \left\{ - \left(\frac{2\Delta-d}{2\ell^d} \right) \left(\frac{\ell}{\ell'} \right)^{2\Delta-d} \left(\varphi_\ell - \left(\frac{\ell}{\ell'} \right)^{d-\Delta} \varphi_{\ell'} \right)^2 \right\}. \quad (31)$$

This time, the shift towards $\varphi_{\ell'}$ and the width compete: both are order $\sim \ell^{d-\Delta}$. It follows that the variables maintain an order one correlation, even in the limit $\ell \rightarrow 0$. In alternate quantization, we conclude that EAdS has memory.⁵

As expected, these results mirror that of the “fast-falloff” and “slow-falloff” branches on the Gaussian tree of section 2.2, and the second-eigenvalue condition discussed in the Ising tree of section 2.1. Here, standard quantization implies a falloff with characteristic dimension greater than $d/2$, and doesn’t permit memory. Alternate quantization implies a falloff slower than $d/2$, and maintains memory.

⁵One might wonder what happens at the point where $\Delta = d/2$. There, one can check that both “standard” and “alternate” conditions are forgetful, since the width is proportional to $\ell^{d/2}$, and the shift is proportional to $\ell^{d/2}/\log \ell$.

2.3.3 Mutual information

So far, we have treated only the spatial zero mode and been somewhat binary in the distinction between memory and forgetfulness. In this section, we will be a little more quantitative. We'll consider a general Fourier component $\varphi_{\mathbf{k}}(z)$, and compute the mutual information $I(\varphi_{\mathbf{k}}(\ell); \varphi_{\mathbf{k}}(\ell'))$ between the mode at some fixed radius ℓ' in the bulk of EAdS, and the same mode, evaluated at a radius ℓ that approaches the boundary.

The mutual information of two random variables is defined as the sum of the differential entropies of the marginal distributions, minus the entropy of the joint distribution:

$$I(X; Y) = S(X) + S(Y) - S(X, Y). \quad (32)$$

Here, the differential entropy S is defined as the integral of $-p(x) \log p(x)$, and can be positive or negative. To compute the relevant entropies, we need the marginal distributions for $\varphi_{\mathbf{k}}(\ell)$ and $\varphi_{\mathbf{k}}(\ell')$, as well as the joint distribution for both. To compute the marginal distribution, we divide the bulk path integral up into IR and UV pieces, and take

$$P(\varphi_{\mathbf{k}}(\ell)) = \mathcal{N} \Psi_{UV}(\varphi_{\mathbf{k}}(\ell)) \Psi_{IR}(\varphi_{\mathbf{k}}(\ell)). \quad (33)$$

Here, \mathcal{N} is a normalization constant, and the IR wave function is a path integral over field configurations that are smooth in the interior of the space, and match onto $\varphi_{\mathbf{k}}(\ell)$ at radius ℓ . As always, we evaluate the various path integrals by evaluating the action on the relevant classical solutions, which are linear combinations of the Bessel functions $I_{\pm\nu}(kz)$, where

$$\nu = \Delta - \frac{d}{2} = \frac{1}{2} \sqrt{d^2 + 4m^2}. \quad (34)$$

A straightforward but somewhat tedious evaluation gives the marginal distribution for alternate boundary conditions as

$$P(\varphi_{\mathbf{k}}(\ell)) = \mathcal{N} \exp \left\{ -\frac{1}{2\ell^d} \frac{\varphi_{\mathbf{k}}(\ell)^2}{I_{-\nu}(k\ell) K_{\nu}(k\ell)} \right\} \quad (\text{alternate quant.}) \quad (35)$$

and for standard boundary conditions as

$$P(\varphi_{\mathbf{k}}(\ell)) = \mathcal{N} \exp \left\{ -\frac{1}{2\ell^d} \frac{\varphi_{\mathbf{k}}(\ell)^2}{I_{\nu}(k\ell) K_{\nu}(k\ell)} \right\} \quad (\text{standard quant.}). \quad (36)$$

The expression for the joint distribution is slightly more complicated. In addition to the UV and IR wave functions, one has to compute a VI wave function that implements the path integral over $\ell < z < \ell'$, and then take the product of all three,

$$P(\varphi_{\mathbf{k}}(\ell), \varphi_{\mathbf{k}}(\ell')) = \mathcal{N} \Psi_{UV}(\varphi_{\mathbf{k}}(\ell)) \Psi_{VI}(\varphi_{\mathbf{k}}(\ell), \varphi_{\mathbf{k}}(\ell')) \Psi_{IR}(\varphi_{\mathbf{k}}(\ell')). \quad (37)$$

This joint distribution is Gaussian, but the covariance matrix is an unpleasant combination of Bessel functions. The mutual information, however, simplifies rather nicely. For the alternate boundary conditions, we find

$$I(\varphi_{\mathbf{k}}(\ell); \varphi_{\mathbf{k}}(\ell')) = -\frac{1}{2} \log \left(1 - \frac{I_{-\nu}(k\ell) K_{\nu}(k\ell')}{I_{-\nu}(k\ell') K_{\nu}(k\ell)} \right) \quad (\text{a.q.}), \quad (38)$$

while for the regular boundary conditions, we get

$$I(\varphi_{\mathbf{k}}(\ell); \varphi_{\mathbf{k}}(\ell')) = -\frac{1}{2} \log \left(1 - \frac{I_{\nu}(k\ell) K_{\nu}(k\ell')}{I_{\nu}(k\ell') K_{\nu}(k\ell)} \right) \quad (\text{s.q.}). \quad (39)$$

In the limit of small ℓ , the mutual information for regular boundary conditions tends to zero as $(k\ell)^{2\nu}$, as shown in the right panel of figure 3. On the other hand, with alternate boundary conditions, we find a nonzero limit

$$I(\varphi_{\mathbf{k}}(0); \varphi_{\mathbf{k}}(\ell')) = \frac{1}{2} \log \left(\frac{I_{-\nu}(k\ell')}{I_{\nu}(k\ell')} \right) \quad (\text{a.q.}). \quad (40)$$

This mutual information is plotted as a function of ν in the left panel of figure 3. There

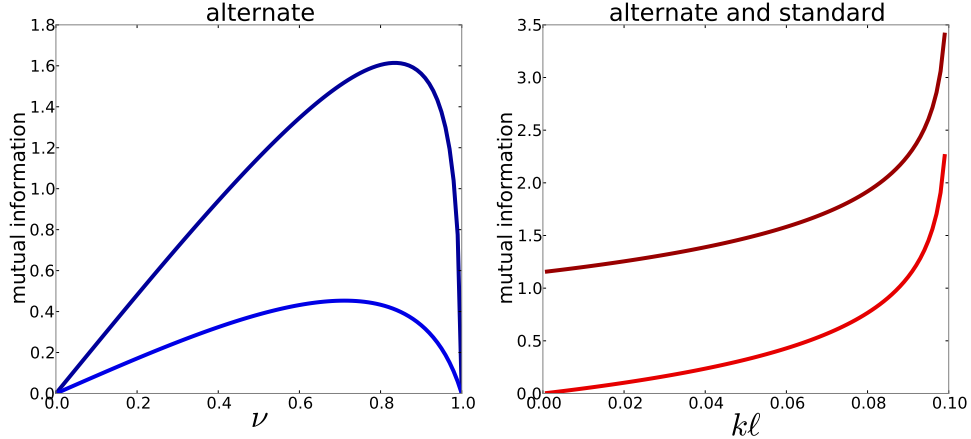


Figure 3: (Left) the mutual information $I(\varphi_{\mathbf{k}}(\ell); \varphi_{\mathbf{k}}(\ell'))$ for alternate quantization, considered as a function of ν . In this plot, ℓ has been taken to zero, while $k\ell' = 0.1$ in the top line, and 0.5 in the bottom line. (Right) the mutual information for both boundary conditions, with ν fixed at 0.5 and $k\ell'$ fixed at 0.1, plotted as a function of $k\ell$. The upper line is alternate, and the lower is standard.

are two interesting points as a function of ν . First, at $\nu = 0$, which is equivalent to $\Delta = d/2$, the mutual information is exactly zero, consistent with the zero-mode analysis above. Second, the mutual information also vanishes at the lower end of the alternate quantization window, $\nu = 1$, which corresponds to the unitarity bound $\Delta_- = (d - 2)/2$.

2.4 Free fields in dS

In de Sitter space, we will set up the memory question in a manner that is now familiar, by studying the zero mode of a massive scalar, and perturbing the initial condition away from Bunch-Davies. Then we will ask whether the late-time statistics of the zero mode is correlated with the choice of initial condition.

Of course, a free field in de Sitter is somewhat different from the EAdS and tree models we studied so far. It is a Lorentzian quantum mechanical system, subject to the constraint of unitarity. For free theories, this constraint is particularly strong, since the different modes decouple, and the evolution of each mode must be unitary. This means that information about the initial conditions for the zero mode can't get scrambled into phase correlations between various modes. Indeed, we'll see that Fourier components of free fields in de Sitter maintain memory of initial conditions for any allowed mass. Cosmic no-hair applies to local quantities in position space, but not to global quantities like Fourier modes.

The metric for the flat slicing of de Sitter space is

$$ds^2 = \frac{-d\eta^2 + dx^i dx^i}{\eta^2} \quad i = 1, \dots, d, \quad (41)$$

where η plays the role of conformal time and the future boundary is at $\eta = 0$. As in EAdS, the wave equation has two branches, characterized by different falloff behaviors at late time $\sim \eta^{\Delta_+}$ and $\sim \eta^{\Delta_-}$ where the de Sitter dimensions are

$$\Delta_{\pm} = \frac{1}{2} \left(d \pm \sqrt{d^2 - 4m^2} \right). \quad (42)$$

The quantum state of the field at conformal time η is described by a wave function $\Psi[\phi(\mathbf{x}); \eta]$. We will specialize to the spatial zero mode, denoted $\varphi(\eta)$, and the corresponding wave function $\Psi(\varphi, \eta)$. Expectation values of functions of φ are computed using the weighting $|\Psi|^2$. Normally, in de Sitter space, one uses the Bunch-Davies ground state wave function, which is computed in appendix A. To test for memory, we'll change the initial condition by constraining the initial value of the zero mode φ at some early time η' .

Specifically, we'll take a wave packet at initial time η' , and compute the wave function at late time η using the Gaussian propagator.

$$\Psi(\varphi_\eta, \eta) = \int d\varphi K(\varphi_\eta, \varphi; \eta, \eta') \exp \left\{ -A (\varphi_{\eta'} - \varphi)^2 \right\} \quad (43)$$

The propagator K can be computed by evaluating the action on the appropriate classical solution. Alternatively, it is simply the analytic continuation of the wave function Ψ_{VI}

from the previous subsection. Up to normalization, $K(\varphi_\eta, \varphi; \eta, \eta')$ has the leading behavior

$$\exp \left\{ i \left(\frac{\Delta_-}{2\eta^d} \right) \varphi_\eta^2 + i \left(\frac{2\Delta_- - d}{2\eta^d} \right) \left(\frac{\eta}{\eta'} \right)^{2\Delta_+ - d} \varphi_\eta^2 + i \left(\frac{2\Delta_+ - d}{\eta^d} \right) \left(\frac{\eta}{\eta'} \right)^{\Delta_+} \varphi_\eta \varphi - i \frac{\Delta_+}{2\eta^d} \varphi^2 \right\}. \quad (44)$$

First, let's take the almost massless case where Δ_- is real and less than $d/2$. Then, doing the Gaussian integrals and taking the modulus-squared, we find the probability distribution

$$P(\varphi_\eta) \sim \exp \left\{ - \frac{\alpha}{\eta^{2\Delta_-}} (\varphi_\eta - \eta^{\Delta_-} \beta \varphi_{\eta'})^2 \right\} \quad (45)$$

$$\alpha \equiv \frac{2A\eta'^{2\Delta_- - d}}{4A^2 + \Delta_+^2} (2\Delta_+ - d)^2 \quad \beta \equiv \frac{\Delta_+}{2\Delta_+ - d}.$$

Here, to review the notation, φ_η is the configuration at late time $\eta \rightarrow 0$, and $\varphi_{\eta'}$ is the center of the Gaussian wave packet that defines the initial conditions at early time η' . The key point is that the width of the distribution for φ_η and the shift in the direction of $\varphi_{\eta'}$ are both of order $\sim \eta^{\Delta_-}$. This means that φ_η remains significantly biased in the direction of the initial conditions, so the system has memory.

The case of $\Delta_\pm = d/2$ and complex Δ_\pm need to be treated separately. First, for complex Δ_\pm , the real part is always $d/2$. A straightforward calculation similar to the above demonstrates that the shift oscillates with scale, but the decay of its envelope matches the decay of the width, and both are proportional to $\eta^{d/2}$. For $\Delta_\pm = d/2$, the shift and width are also matched, proportional to $\sim \eta^{d/2} \log \eta$. We see that a free massive scalar in dS has memory for all allowable values of Δ_\pm .

Even without the unitarity argument or the explicit calculation, the results for $\Delta_- < d/2$ could have been anticipated from the analogy to the Ising model and the Kesten-Stigum lower bound. Free fields in de Sitter can be modeled by a stochastic Markov system [18], and $\Delta_- < d/2$ implies a second eigenvalue greater than the critical value.⁶

2.5 CFT

Since we defined memory in terms of fluctuation statistics near the boundary of (EA)dS, we should be able to translate the forgetful transition into CFT terms. In this section, we will do this in two related ways. First, we'll consider the statistics of certain sums of operators in the fixed point theory and argue that bulk memory is related to a failure of

⁶Interacting theories in de Sitter can have a falloff faster than $\Delta_- = d/2$ [19]. It seems likely that, in such theories, memory of initial conditions is not recorded in the statistics of simple late-time quantities.

the central limit theorem. Second, we'll mock up modified bulk initial conditions as an RG transient and look for memory in the UV. In both cases, we'll find a sharp change of behavior at $\Delta = d/2$.

Consider, then, a CFT in d dimensions, and focus on a patch of volume L^d , with a lattice cutoff at scale ϵ . Choose an operator O_i with dimension Δ_i , and define the variable

$$M_\epsilon = \sum_x O_i(x). \quad (46)$$

This sum contains one term per lattice point in the patch, for a total of $(L/\epsilon)^d$ summands, so as the lattice becomes small, the quantity M_ϵ involves a very large number of operators. This quantity is analogous to the Ising magnetization at level u in the tree, with $p^{-u} \sim \epsilon/L$. Based on the second-eigenvalue condition, we expect the existence of memory to be connected with a transition as a function of Δ_i . Specifically, we expect that for $\Delta_i > d/2$, small ϵ will make the distribution $P(M_\epsilon)$ Gaussian, while for $\Delta_i < d/2$ the distribution will remain non-Gaussian in the limit of small ϵ .

To confirm this, we will inspect some moments of the distribution for M_ϵ . The two point function is

$$\langle M_\epsilon^2 \rangle = \sum_{x,y} \langle O_i(x) O_i(y) \rangle. \quad (47)$$

We can use translation invariance (ignoring a small correction due to finite volume) to do one of the sums,

$$\langle M_\epsilon^2 \rangle \approx \frac{L^d}{\epsilon^d} \sum_x \langle O_i(x) O_i(0) \rangle. \quad (48)$$

First, suppose $\Delta_i > d/2$. Then, the remaining sum is UV divergent, and the leading contribution is just the two point function at lattice scale. We normalize the operators so this is one, making the overall answer proportional to $(L/\epsilon)^d$.

Next, suppose $\Delta_i < d/2$. Then the sum is dominated by the IR, so it can be approximated as an integral

$$\int_0^L \frac{d^d x}{\epsilon^d} \frac{\epsilon^{2\Delta_i}}{|x|^{2\Delta_i}} \sim \frac{L^{d-2\Delta_i}}{\epsilon^{d-2\Delta_i}}.$$

This means the two point function is proportional to $(L/\epsilon)^{2d-2\Delta_i}$. To get a nicely normalized quantity in the continuum limit, we should divide M_ϵ not by the square root of the number of points, but by a fractional power, $M_\epsilon(\epsilon/L)^{d-\Delta_i}$.

To go further, consider the fourth moment,

$$\langle M_\epsilon^4 \rangle = \sum_{x,y,z,w} \langle O_i(x) O_i(y) O_i(z) O_i(w) \rangle. \quad (49)$$

This is a four-point function, which depends on the entire operator spectrum of the theory. However, for $\Delta_i > d/2$, it is dominated by UV singularities when two pairs of the operators approach each other. There are three ways the operators can pair up, so, for large L/ϵ

$$\langle M_\epsilon^4 \rangle = 3 \langle M_\epsilon^2 \rangle \langle M_\epsilon^2 \rangle. \quad (50)$$

This equation implies that the fourth order cumulant is zero, consistent with Gaussian statistics. Suppose, instead, that $\Delta_i < d/2$. Then there are no coincident-point divergences in the sum. It follows from scaling that result has to be proportional to $(L/\epsilon)^{4d-4\Delta_i}$. The coefficient depends on the OPE constants and spectrum of the theory, so, in general, the fourth-order cumulant will be nonzero.

Perhaps a more direct way to understand memory in a CFT is to study an RG transient, rather than focusing on the fixed point statistics. A related issue was considered in [20], and we will use a similar construction. Specifically, we will mock up the bulk transient by adding an operator O_i to the action, far from our patch of size L^d .⁷ Let us arrange the coefficient so that one point function of O_i at the center of the patch, and renormalized at scale L , is order one. Within the patch, this means that the one point function of the operator $O_i(x)$ at the lattice scale is order $(\epsilon/L)_i^\Delta$, so the operator M_ϵ will have a one-point function of order $(\epsilon/L)^{\Delta_i-d}$. Comparing this to the variance of the distribution for M_ϵ in the unperturbed CFT, we find that the statistics of M_ϵ can detect the perturbation if $\Delta_i < d/2$, but not if $\Delta_i > d/2$.

3 Configuration-space ultrametricity

In this section, we will review the connection between memory and the existence of multiple extreme (pure) components in the Gibbs state. We will discuss the branching structure of the space of pure states for the Ising model. We will then switch to de Sitter, where Anninos and Denef argued that, similarly, the Bunch-Davies vacuum splits into a tree-like space of extreme states [13]. We'll generalize their analysis to positive mass.

⁷We are not smearing the operator over the L^d patch as in [20]; we are inserting the operator at a definite location far away. Had we smeared the operator, we would have found an effect that becomes large in the UV for irrelevant O_i , unlike the bulk transient we are trying to model. We are grateful to Stephen Shenker for a discussion of this point.

3.1 Ising model on a tree

Mathematically, memory in the Ising model is connected to the existence of nontrivial variables “at infinity” in the tree. As an example, we can consider the appropriately normalized total magnetization at generation u . For $\lambda > 1/\sqrt{p}$, the limit theorems of [8] (see [7] or [21] for explanation) establish that the variables

$$\frac{M_u}{(p\lambda)^u} \quad (51)$$

converge to a random variable M_∞ , which is correlated with the spin at the root of the tree. Let us contrast this with the case in the no-memory phase $\lambda \leq 1/\sqrt{p}$. There, the marginal distributions for the variables

$$\frac{M_u}{p^{u/2}} \quad (52)$$

converge to a Gaussian with mean zero, but the variables themselves do not converge: in a given realization of the spin system, the variable M_u would continue switching sign as a function of u .

In probability theory, the concept of variables at infinity is formalized as the tail field, which is the set of observables in an infinite system that don’t depend on the variables at any finite number of sites. A system is described as having a trivial tail if every tail event has probability either zero or one. The existence, in the memory phase, of correlation between the variable M_∞ and the root implies that the distribution for M_∞ has finite width, so the tail field is nontrivial. This is equivalent (see [22], Theorem 7.7) to the statement that the free boundary Gibbs state is not an extreme point in the convex space of Gibbs states.⁸

We would like to characterize the space of the extreme Gibbs states. For the Ising model, we can get a fairly complete picture of the space of these as follows. First, we divide up the ensemble according to whether the variable M_∞ is positive or negative, in other words, we divide it up according to whether the reconstruction of the initial spin is up or down. This cleanly divides the set of extreme components that makes up Gibbs state into two components. We can repeat this procedure for tail variables corresponding to the total magnetization associated to the leaves of the subtrees emanating from the p children of the root. Focus on the $p = 2$ case for simplicity. The root has two children at level $u = 1$, which we’ll label $(1, 1)$ and $(1, 2)$. Let $M_\infty^{(1,1)}$ and $M_\infty^{(1,2)}$ denote the rescaled

⁸Extreme (pure) states and their connection with spin glasses was recently reviewed in [23].

magnetization at infinity for the subtrees associated to these vertices. If M_∞ is positive, then there are three possibilities: both $M_\infty^{(1,1)}$ and $M_\infty^{(1,2)}$ might be positive, or they could have opposite sign. Similarly, if M_∞ is negative, then both might be negative or they might have opposite signs. Proceeding in this way, we can further divide the Gibbs state according to the 2^{p^u} possible signs of the p^u variables $M_\infty^{(u,i)}$, $i = 1, \dots, p^u$, where $M_\infty^{(u,i)}$ is the total magnetization at infinity in the subtrees growing out of the i -th vertex at generation u .

As a function of u , this decomposition defines a branching, RG-type evolution of the space of pure states. Because of the existence of memory, the sign of the variable $M_\infty^{(u,i)}$ is correlated with the i -th spin at generation u in the tree, so this evolution is related to the evolution of the configurations in the actual system. In the limit of small γ , this relation becomes exact, but at finite γ it is approximate, since the reconstruction of the spin (u, i) from $M_\infty^{(u,i)}$ can be wrong.

3.2 Free fields in dS

Anninos and Denef recently suggested a very similar extreme state decomposition for the Bunch-Davies vacuum associated to a massless field in de Sitter [13]. Related overlap distributions were also computed in [24]. Part of the motivation for invoking extreme states was the failure of the massless field to cluster; the two point correlator is logarithmically divergent at large distance. By contrast, the two point function of free massive fields clusters, so one might guess that the analysis of [13] is related to a pathology of the massless scalar. This is not the case. In the remainder of this section, we will compute overlap distributions for positive mass fields in de Sitter. We'll see that the ultrametric tendency of the massless field is shared by massive fields as long as $\Delta_- < d/4$.

3.2.1 Setup

As in section 2.4, we will work with de Sitter space in flat slicing, but we'll make the IR cutoff explicit by compactifying space on a torus of comoving size L , $x^i \sim x^i + L$. The probability distribution on spatial field configurations is given by the norm-squared of the wave function, $|\Psi|^2$. Following Anninos and Denef, we will define a distance on the space of these configurations,

$$d(1, 2) = \frac{1}{L^d} \int d^d x \left(\hat{\phi}_1(\mathbf{x}) - \hat{\phi}_2(\mathbf{x}) \right)^2, \quad (53)$$

where $\hat{\phi}$ is obtained from ϕ by subtracting the zero mode and smearing over a comoving scale corresponding to a large but fixed number of horizons. It will be convenient to define a regulated distance $\delta(1, 2)$ by subtracting the mean,

$$\delta(1, 2) = d(1, 2) - \langle d(1, 2) \rangle. \quad (54)$$

Of course, this subtracted distance can be either positive or negative.

We will be interested in the following questions [13]: what is the probability, in the ensemble of fluctuations determined by Ψ , that two independently chosen configurations have a given distance δ ? Or that three configurations will have distances $\delta_1, \delta_2, \delta_3$? Rather than computing the probability distribution for $\delta(1, 2)$ directly, it is easier to compute exponential moments $\langle e^{-s\delta(1,2)} \rangle$ over field configurations ϕ_1 and ϕ_2 , as a function of s , and recover the distribution for δ by inverse Laplace transform

$$P_\eta(\delta) \propto \int_{-i\infty}^{i\infty} e^{s\delta} \langle e^{-s\delta(1,2)} \rangle_\eta ds. \quad (55)$$

The expectation value $\langle \cdot \rangle_\eta$ is done with respect to the measure $|\Psi|^2$ at time η , provided by the Bunch-Davies wave function. This wave function is computed in appendix A, and the result, for superhorizon modes $k\eta \ll 1$, is

$$|\Psi(\phi, \eta)|^2 = \mathcal{N} \exp \left(-2 \sum_{\mathbf{k}} \beta(k, \eta) |\varphi_{\mathbf{k}}|^2 \right) \quad (56)$$

where \mathcal{N} is a normalization factor, independent of ϕ , $k = |\mathbf{k}|$ and

$$\beta(k, \eta) \sim \frac{L^d \ell_{dS}^{d-1}}{\eta^{2\Delta_-}} k^{d-2\Delta_-} \quad \Delta_- = \frac{1}{2} \left(d - \sqrt{d^2 - 4m^2 \ell_{dS}^2} \right). \quad (57)$$

The proportionality constant in the definition of β is an order one number that depends on $m\ell_{dS}$ and d . It is given in the appendix but won't be needed here.

The wave function is a product over the different \mathbf{k} modes, and the distance distribution is quadratic in ϕ_1 and ϕ_2 , so we can compute the expectation value $e^{-s\delta(1,2)}$ by Gaussian integration, mode by mode. The computation is entirely parallel to the massless one detailed in [13], and the result is

$$\langle e^{-s\delta(1,2)} \rangle_\eta = \prod'_{\mathbf{k} \neq 0} \frac{e^{s/\beta(k, \eta)}}{1 + s/\beta(k, \eta)}, \quad (58)$$

where the primed product runs over unordered pairs $(\mathbf{k}, -\mathbf{k})$ with $\mathbf{k} \neq 0$. Similarly, the probability distribution for the distances between three configurations is given by a three

dimensional Laplace transform of

$$\begin{aligned} & \langle e^{-s_1 \delta(1,2) - s_2 \delta(1,3) - s_3 \delta(2,3)} \rangle_\eta \\ &= \prod_{\mathbf{k} \neq 0}' \frac{e^{(s_1 + s_2 + s_3)/\beta(k, \eta)}}{1 + (s_1 + s_2 + s_3)/\beta(k, \eta) + 3(s_1 s_2 + s_1 s_3 + s_2 s_3)/4\beta(k, \eta)^2}. \end{aligned} \quad (59)$$

If the mass is zero, then the Gaussian kernel β is independent of conformal time η and we can take the late-time limit safely. However, in the massive case, $\Delta_- > 0$, and β blows up at late time. This means that the exponential moments tend to zero for any fixed s , and the distance distribution collapses to a delta function.

This is a reflection of the fact that massive fields in de Sitter space have a power law fade at late time, proportional to η^{Δ_-} . We can compensate for this by defining a new, η -dependent metric on field configurations,⁹

$$\begin{aligned} d_\Delta(1, 2) &= \begin{cases} \left(\frac{L}{\eta}\right)^{2\Delta_-} \frac{c}{L^d} \int d^d \mathbf{x} \left(\hat{\phi}_1(\mathbf{x}) - \hat{\phi}_2(\mathbf{x})\right)^2 & \text{for } \Delta_- < \frac{d}{4} \\ \left(\frac{L}{\eta}\right)^{d/2} \frac{c'}{L^d} \int d^d \mathbf{x} \left(\hat{\phi}_1(\mathbf{x}) - \hat{\phi}_2(\mathbf{x})\right)^2 & \text{for } \Delta_- > \frac{d}{4} \end{cases} \\ \delta_\Delta(1, 2) &= d_\Delta(1, 2) - \langle d_\Delta(1, 2) \rangle. \end{aligned} \quad (60)$$

The reason for the change in behavior of the normalization at $\Delta_- = d/4$ will be made clear below, where we'll see explicitly that the above definition ensures that the width of the distribution for $\delta_\Delta(1, 2)$ has a finite and nonzero late-time limit. In what follows, we'll adjust the constants of proportionality c, c' as a function of mass so that the variance is one.

3.2.2 Ultra-light fields

We'll begin by considering the case $\Delta_- < d/4$, corresponding to a very small mass $(m\ell_{dS})^2 < 3d^2/16$. In this mass range, the explicit power of conformal time in the definition of $\delta_\Delta(1, 2)$ cancels the time-dependence of β . Up to a constant multiple in the definition of δ_Δ , which we fix by measuring distances in units of the variance, we have

$$\langle e^{-s\delta_\Delta(1,2)} \rangle = \prod_{\mathbf{n} \neq 0}' \frac{e^{s/n^{d-2\Delta_-}}}{1 + s/n^{d-2\Delta_-}}, \quad (61)$$

where the primed product runs over unordered pairs $(\mathbf{n}, -\mathbf{n})$, and $n = |\mathbf{n}|$. As long as $\Delta_- < \frac{d}{4}$, this product converges, and we are able to remove the smearing function that cuts off high momentum modes. A similar formula holds for the triple overlap.

⁹For $\Delta_- = d/4$, an additional factor of $1/\log(L/\eta)$ is required in the normalization

As far as we know, this infinite product (61) is not known in closed form. One could approximate the product as the exponential of the integral of the logarithm, which can be evaluated in terms of known functions. But, even with this simplification, it doesn't seem possible to perform the Laplace transform to recover $P(\delta)$, even in the saddle point approximation.

However, even without doing the relevant integrals, it is clear that the distributions are continuous in Δ_- near 0, so that the overlap distributions for ultra-light fields match smoothly to the massless distributions as $m\ell_{dS} \rightarrow 0$. This establishes that the ultrametricity of [13] extends to very small mass.

Also, we can get a qualitative picture by studying the distributions numerically. The products are easy to compute, but the oscillatory Laplace transform is inconvenient. Instead, we do the transform approximately by numerically searching for saddle points. As a first example, dS_{1+1} probability distributions for a single distance $\delta_{\Delta}(1, 2)$ are shown in Figure 4. For zero mass, we recover the Gumbel distribution of [13]. As the mass-squared

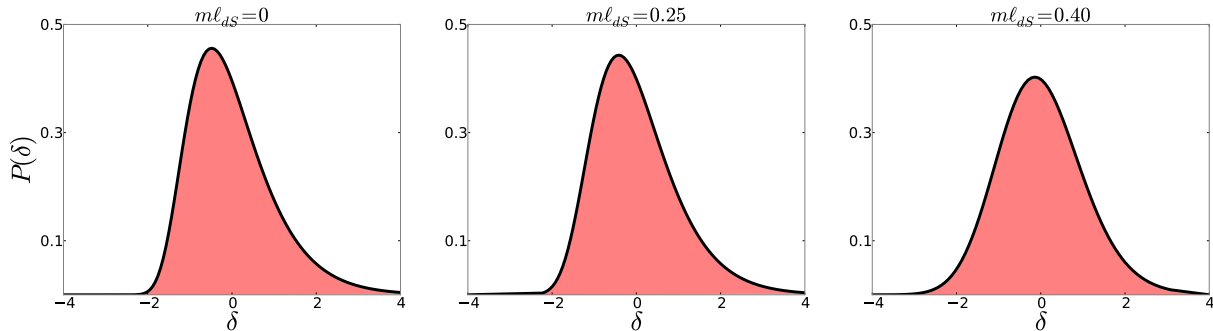


Figure 4: Saddle point approximations of dS_{1+1} overlap distributions, measured in units of the variance, for three different values of the mass. $\Delta_- = d/4$ corresponds to $m\ell_{dS} = 0.43$.

increases towards the critical value $3d^2/16$, we see the lopsidedness fading as the Gumbel turns into a Gaussian.

To check for ultrametricity, we need to evaluate the triple overlap distribution, $P(\delta_1, \delta_2, \delta_3)$. The ultrametricity of [13] shows itself when one distance is small, by preferring that the other two distances be equal. To check for this behavior, we plot a conditional probability, $P(\delta | 2, -3)$ in Figure 5. If the distribution were truly ultrametric, this would be a delta function enforcing $\delta = 2$. And, indeed, for zero mass, the distribution is rather peaked near $\delta = 2$. As the mass increases from zero, the peak near $\delta = 2$ broadens and moves left towards some kind of non-ultrametric compromise between -3, 0, and 2.

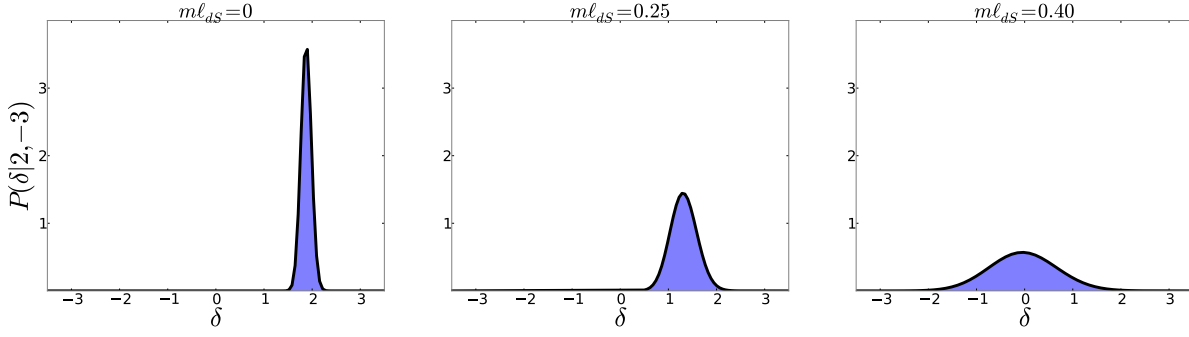


Figure 5: Saddle point approximations of dS_{1+1} conditional probability $P(\delta|2, -3)$, measured in units of the variance of the corresponding double overlap distributions, for three different values of the mass. Again, the critical mass is $m\ell_{dS} = 0.43$.

It is worth emphasizing that the conditional probability plotted is *very* conditional, in the sense that the absolute probability for having any of the three distances equal to -3 is extremely small. This is apparent in Figure 4. To see the sharp ultrametric peaking, we are forced to evaluate the triple overlap distribution in a very rare region of parameter space. If, instead, we were to plot $P(\delta|2, -1)$, we would find little or no evidence of ultrametricity.

3.2.3 Heavier fields

We now turn to non-ultra-light fields, for which $\Delta_- \geq d/4$. For such fields, the scaling factor in (60) has a different form. The reason is that the infinite product (61) diverges, so we can't naively remove the smearing cutoff on the field modes. Instead, we regulate the product with a comoving cutoff on momentum that is a large but fixed multiple of $1/\eta$. With this prescription, one can check that the definition (60) ensures a finite late-time limit for the distance distribution.

In fact, the calculation simplifies rather dramatically, because the product is dominated by the most ultraviolet modes. In the late-time limit, we find

$$\langle e^{-s\delta_{\Delta}(1,2)} \rangle = e^{s^2/2}, \quad (62)$$

and a similar Gaussian formula for the moments of the triple-overlap distribution. The Laplace transforms are simple, giving $P(\delta)$ as a Gaussian. Normalizing the variance to one, we find the triple-overlap distribution

$$P_{\Delta_- \geq d/4}(\delta_1, \delta_2, \delta_3) = \frac{2}{3\sqrt{3\pi^3}} \exp \left(-\frac{5}{9} (\delta_1^2 + \delta_2^2 + \delta_3^2) + \frac{2}{9} (\delta_1\delta_2 + \delta_1\delta_3 + \delta_2\delta_3) \right). \quad (63)$$

The conditional probability for δ_1 , given δ_2 and δ_3 is a Gaussian, peaked at $\delta_1 = \frac{\delta_2 + \delta_3}{5}$. In particular, if $\delta_2 = -\delta_3$, the conditional probability for δ_1 is symmetric and peaked at zero. This lack of attraction towards the larger of the two other distances provides a sharp criterion for the absence of ultrametricity for $\Delta_- \geq d/4$. Based on the first half of this paper, one might expect the transition to happen at $\Delta_- = d/2$, not $\Delta_- = d/4$. Apparently, memory is necessary for non-Gaussianity of the Anninos-Denef overlap distributions, but not sufficient.¹⁰

4 Conclusion

Memory is defined as the existence of correlation between global variables at infinity and local variables at some finite point. A well-studied memory/forgetfulness transition happens in the Ising model on the tree, suggesting a critical value of the dimension $\Delta = d/2$ for fluctuating dynamics in (EA)dS. Indeed, we found:

- Free fields in EAdS with standard quantization have $\Delta \geq d/2$ and forget perturbations deep in the bulk. However, with alternate quantization, the dimension can be less than $d/2$, and global variables at the boundary remain sensitive to such perturbations.
- Free fields in dS never fall off faster than $\Delta = d/2$. Despite local cosmic no-hair, global memory always exists.
- The transition at $d/2$ can be understood in boundary CFT terms without assuming a free theory.

We discussed the extreme states implied by the existence of memory in such systems. In de Sitter, we find that the ultrametric structure of these states persists to finite positive mass but disappears at $\Delta_- = d/4$. Memory is necessary but not sufficient for ultrametricity.

Acknowledgments

We would like to thank Dionysios Anninos, Frederik Denef, and Ben Freivogel for insights about ultrametricity at positive mass, Max Kleiman-Weiner for discussion of reconstruction, Persi Diaconis and Allan Sly for help with the mathematical literature, and Stephen

¹⁰Numerical exploration suggests that this conclusion is robust to changing the distance metric used to e.g. an L_1 instead of an L_2 norm.

Shenker for comments on the CFT interpretation. We are grateful to Dionysios Anninos and Frederik Denef for organizing “Cosmology and Complexity 2012,” the productive and refreshing workshop at which this work began. D.S. supported by the NSF under the GRF program, by NSF grant 0756174 and by the Stanford Institute for Theoretical Physics. D.A.R. is supported by the DOD through the NDSEG Program, by the Fannie and John Hertz Foundation, and is grateful to the SITP for hospitality during the final stages of this work. This work was supported in part by the U.S. Department of Energy under cooperative research agreement Contract Number DE-FG02-05ER41360.

A Super-horizon wave function in de Sitter space

In this appendix, we review the calculation of the super-horizon wave function for a free massive field in the Bunch-Davies vacuum of de Sitter space, following [25] and [17]. The wave function Ψ depends on the spatial field $\phi(\mathbf{x})$, or its Fourier transform $\varphi_{\mathbf{k}}$, at a given conformal time η_0 . It is given by a path integral over field configurations that satisfy a vacuum condition in the asymptotic past, and are equal to $\phi(\mathbf{x})$ at time η_0 . As always in Gaussian theories, we can do this path integral by evaluating the action on the appropriate solution $\phi(\mathbf{x}, \eta)$ of the equations of motion,

$$\Psi[\eta_0, \phi(\mathbf{x})] \propto e^{-iS_{cl}[\phi(\mathbf{x}, \eta)]}. \quad (64)$$

As the in the main body of the paper, we’ll work in flat slicing, with metric

$$ds^2 = \ell_{dS}^2 \frac{-d\eta^2 + dx^i dx^i}{\eta^2} \quad i = 1, \dots, d, \quad (65)$$

with ℓ_{dS} the de Sitter radius and $-\infty < \eta < 0$. With this metric, the action for a free massive scalar is

$$S = \frac{\ell_{dS}^{d+1}}{2} \int \frac{d^d \mathbf{x} d\eta}{\eta^d} \left\{ \frac{\eta^2}{\ell_{dS}^2} (\partial_\eta \phi)^2 - \frac{\eta^2}{\ell_{dS}^2} (\partial_i \phi)^2 - m^2 \phi^2 \right\}. \quad (66)$$

As before, we will introduce an explicit IR cutoff by making the identification $x^i \sim x^i + L$. This allows us to decompose the field into spatial Fourier components, $\phi(\eta, \mathbf{x}) = \varphi_{\mathbf{k}}(\eta) e^{i\mathbf{k} \cdot \mathbf{x}}$ with quantized $\mathbf{k} = \frac{2\pi \mathbf{n}}{L}$. The equations of motion decouple into equations for each \mathbf{k}

$$\partial_\eta^2 \varphi_{\mathbf{k}} - \frac{d-1}{\eta} \partial_\eta \varphi_{\mathbf{k}} + \left(\frac{m^2 \ell_{dS}^2}{\eta^2} + k^2 \right) \varphi_{\mathbf{k}} = 0. \quad (67)$$

This differential equation is related to Bessel’s equation and has the general solution

$$\varphi_{\mathbf{k}}(\eta) = \eta^{d/2} (A_1 H_\nu^{(1)}(k\eta) + A_2 H_\nu^{(2)}(k\eta)) \quad (68)$$

$$\nu = \frac{1}{2}\sqrt{d^2 - 4m^2\ell_{dS}^2} = \frac{d}{2} - \Delta_-, \quad (69)$$

where $H_\nu^{(1)}(k\eta)$ and $H_\nu^{(2)}(k\eta)$ are Hankel functions.

One linear combination of A_1 and A_2 is fixed by requiring that at time η_0 , the solution should be equal to the Fourier transform of the argument of the wave function, $\varphi_{\mathbf{k}}$. Fixing the other linear combination amounts to making a choice of vacuum. We pick the Bunch-Davies vacuum [26], also known as Hartle-Hawking [27], Euclidean or adiabatic. The prescription is to choose a solution that's purely positive frequency in the asymptotic past, $\eta \rightarrow -\infty$. This condition is made simple by the nice asymptotic properties of the Hankel function,

$$\begin{aligned} \lim_{|x| \rightarrow \infty} H_\nu^{(1)}(x) &\sim e^{ix} \\ \lim_{|x| \rightarrow \infty} H_\nu^{(2)}(x) &\sim e^{-ix}. \end{aligned} \quad (70)$$

We recognize the latter as the positive frequency modes, so the correct solution is

$$\varphi_{\mathbf{k}}(\eta) = \varphi_{\mathbf{k}} \frac{\eta^{d/2} H_\nu^{(2)}(k\eta)}{\eta_0^{d/2} H_\nu^{(2)}(k\eta_0)}. \quad (71)$$

All that remains is to substitute this solution into the action, mode by mode. We can integrate by parts and use the fact that (71) satisfies the equations of motion to reduce the η integral to a boundary term at η_0 .¹¹

$$S_{cl} = \frac{L^d \ell_{dS}^{d-1}}{2} \sum_{\mathbf{k}} \eta_0^{1-d} \varphi_{-\mathbf{k}} \partial_\eta \varphi_{\mathbf{k}}(\eta) \Big|_{\eta=\eta_0}. \quad (72)$$

We can evaluate the derivative using a Hankel function identity

$$\partial_\eta \varphi_{\mathbf{k}}(\eta) \Big|_{\eta=\eta_0} = \left(\frac{d-2\nu}{2\eta_0} + k \frac{H_{\nu-1}^{(2)}(k\eta_0)}{H_\nu^{(2)}(k\eta_0)} \right) \varphi_{\mathbf{k}}. \quad (73)$$

We are interested in the wave function for superhorizon modes, for which $k\eta_0$ is much less than one, and the Hankel functions can be expanded as

$$\begin{aligned} H_\nu^{(2)}(x) &\approx A(\nu)x^\nu + B(\nu)x^{-\nu} \quad (x \ll 1) \\ A(\nu) &\equiv \frac{1 - i \cot \nu\pi}{2^\nu \Gamma[1 + \nu]} \quad B(\nu) \equiv \frac{2^\nu i \Gamma[\nu]}{\pi}. \end{aligned} \quad (74)$$

¹¹A priori, there is also an oscillatory contribution from $\eta \rightarrow -\infty$. We kill this piece in the usual way, by rotating the contour for η slightly. The condition that the early-time mode is positive frequency ensures that this contribution is exponentially suppressed at early imaginary time.

At this point, it is useful to focus on the square of the wave function, $|\Psi|^2$. This allows us to discard real terms in the action, since they contribute only a phase to $e^{-iS_{cl}}$. Using the expansion above, the assumption $\nu > 0$ and Euler's reflection formula for the Γ function, we find

$$Re(-iS_{cl}) = -L^d \ell_{dS}^{d-1} \sum_{\mathbf{k}} \left(\frac{k^{2\nu}}{\eta_0^{d-2\nu}} \right) \varphi_{\mathbf{k}} \varphi_{-\mathbf{k}} \frac{\Gamma[1-\nu]}{2^{2\nu}\Gamma[\nu]} \sin \nu\pi, \quad (75)$$

so that, finally,

$$|\Psi|^2 \sim \exp \left\{ -2 \sum_{\mathbf{k}} \beta(k, \eta_0) |\varphi_{\mathbf{k}}|^2 \right\} \quad (76)$$

$$\beta(k, \eta) = \sin \nu\pi \frac{\Gamma[1-\nu]}{2^{2\nu}\Gamma[\nu]} \left(\frac{L^d \ell_{dS}^{d-1} k^{2\nu}}{\eta^{d-2\nu}} \right) \quad (\nu > 0).$$

References

- [1] G. Gibbons and S. Hawking, ‘‘Cosmological Event Horizons, Thermodynamics, and Particle Creation,’’ *Phys.Rev.* **D15** (1977) 2738–2751.
S. Hawking and I. Moss, ‘‘Supercooled Phase Transitions in the Very Early Universe,’’ *Phys.Lett.* **B110** (1982) 35.
- [2] R. M. Wald, ‘‘Asymptotic behavior of homogeneous cosmological models in the presence of a positive cosmological constant,’’ *Phys.Rev.* **D28** (1983) 2118–2120.
- [3] D. Marolf and I. A. Morrison, ‘‘The IR stability of de Sitter QFT: results at all orders,’’ *Phys.Rev.* **D84** (2011) 044040, [arXiv:1010.5327 \[gr-qc\]](#).
S. Hollands, ‘‘Correlators, Feynman diagrams, and quantum no-hair in deSitter spacetime,’’ [arXiv:1010.5367 \[gr-qc\]](#).
- [4] A. H. Guth, ‘‘The Inflationary Universe: A Possible Solution to the Horizon and Flatness Problems,’’ *Phys.Rev.* **D23** (1981) 347–356.
A. D. Linde, ‘‘A New Inflationary Universe Scenario: A Possible Solution of the Horizon, Flatness, Homogeneity, Isotropy and Primordial Monopole Problems,’’ *Phys.Lett.* **B108** (1982) 389–393.
- [5] For recent reviews of progress in this direction, see below.

- B. Freivogel, “Making predictions in the multiverse,” *Class.Quant.Grav.* **28** (2011) 204007, [arXiv:1105.0244 \[hep-th\]](#).
- M. P. Salem, “Bubble collisions and measures of the multiverse,” *JCAP* **1201** (2012) 021, [arXiv:1108.0040 \[hep-th\]](#).
- [6] W. Evans, C. Kenyon, Y. Peres, and L. J. Schulman, “Broadcasting on trees and the ising model,” *Ann. Appl. Probab.* **10** (2) (2000) 410–433.
- [7] T. Moore and J. L. Snell, “A branching process showing a phase transition,” *Journal of Applied Probability* **16** no. 2, (1979) pp. 252–260.
<http://www.jstor.org/stable/3212894>.
- [8] H. Kesten and B. Stigum, “Additional limit theorems for indecomposable multidimensional galton-watson processes,” *Ann. math. Statist.* **37** (1966) 1463–1481.
- [9] P. Bleher, J. Ruiz, and V. Zagrebnov, “On the purity of the limiting gibbs state for the ising model on the bethe lattice,” *Journal of Statistical Physics* **79** (1995) 473–482. <http://dx.doi.org/10.1007/BF02179399>. 10.1007/BF02179399.
- [10] For reviews of dS, see below.
R. Bousso, “Adventures in de Sitter space,” [arXiv:hep-th/0205177 \[hep-th\]](#).
D. Anninos, “De Sitter Musings,” *Int.J.Mod.Phys.* **A27** (2012) 1230013, [arXiv:1205.3855 \[hep-th\]](#).
- [11] D. Harlow, S. H. Shenker, D. Stanford, and L. Susskind, “Tree-like structure of eternal inflation: A solvable model,” *Phys.Rev.* **D85** (2012) 063516, [arXiv:1110.0496 \[hep-th\]](#).
- [12] P. Breitenlohner and D. Z. Freedman, “Stability in Gauged Extended Supergravity,” *Annals Phys.* **144** (1982) 249.
I. R. Klebanov and E. Witten, “AdS / CFT correspondence and symmetry breaking,” *Nucl.Phys.* **B556** (1999) 89–114, [arXiv:hep-th/9905104 \[hep-th\]](#).
- [13] D. Anninos and F. Denef, “Cosmic Clustering,” [arXiv:1111.6061 \[hep-th\]](#).
- [14] E. Mossel, “Reconstruction on trees: beating the second eigenvalue,” *The Annals of Applied Probability* **11** no. 1, (2001) 285–300.

- [15] A. Zabrodin, “Non-Archimedean strings and Bruhat-Tits trees,” *Commun.Math.Phys.* **123** (1989) 463.
- [16] I. Heemskerck and J. Polchinski, “Holographic and Wilsonian Renormalization Groups,” *JHEP* **1106** (2011) 031, [arXiv:1010.1264 \[hep-th\]](#).
- [17] D. Harlow and D. Stanford, “Operator Dictionaries and Wave Functions in AdS/CFT and dS/CFT,” [arXiv:1104.2621 \[hep-th\]](#).
- [18] A. Starobinsky, “Stochastic de sitter (inflationary) stage in the early universe,” in *Field Theory, Quantum Gravity and Strings*, H. de Vega and N. Sanchez, eds., vol. 246 of *Lecture Notes in Physics*, pp. 107–126. Springer Berlin / Heidelberg, 1986. http://dx.doi.org/10.1007/3-540-16452-9_6.
A. D. Linde, “Eternally Existing Selfreproducing Chaotic Inflationary Universe,” *Phys.Lett.* **B175** (1986) 395–400.
- [19] D. Marolf and I. A. Morrison, “The IR stability of de Sitter: Loop corrections to scalar propagators,” *Phys.Rev.* **D82** (2010) 105032, [arXiv:1006.0035 \[gr-qc\]](#).
- [20] D. Harlow, S. H. Shenker, D. Stanford, and L. Susskind, “The Three Faces of a Fixed Point,” [arXiv:1203.5802 \[hep-th\]](#).
- [21] E. Mossel and Y. Peres, “Information flow on trees,” *Ann. Appl. Probab.* **13 (3)** (2003) 817–844.
- [22] H. Georgii, *Gibbs Measures and Phase Transitions*. de Gruyter, Berlin, 1988.
- [23] F. Denef, “TASI lectures on complex structures,” [arXiv:1104.0254 \[hep-th\]](#).
- [24] M. K. Benna, “De (Baby) Sitter Overlaps,” [arXiv:1111.4195 \[hep-th\]](#).
- [25] J. M. Maldacena, “Non-Gaussian features of primordial fluctuations in single field inflationary models,” *JHEP* **0305** (2003) 013, [arXiv:astro-ph/0210603 \[astro-ph\]](#).
- [26] N. Birrel and P. Davies, *Quantum fields in curved space*. Cambridge Univ. Press, 1982.
- [27] J. Hartle and S. Hawking, “Wave Function of the Universe,” *Phys.Rev.* **D28** (1983) 2960–2975.